

# Piled-cruciform attachment to monopile head reduces deflection

**1 Muhammad Arshad** BSc, MSc, ME, PhD  
Assistant Professor, Department of Geological Engineering,  
University of Engineering and Technology, Lahore, Pakistan;  
formerly PhD candidate, Department of Civil, Structural and  
Environmental Engineering, Trinity College Dublin, Dublin, Ireland  
(corresponding author: arshadm@tcd.ie)

**2 Brendan C. O'Kelly** PhD, FTCD, CEng, CEnv, MICE  
Associate Professor, Department of Civil, Structural and Environmental  
Engineering, Trinity College Dublin, Dublin, Ireland



Much critical infrastructure, including bridges, wind turbine structures, dolphins and some other ocean engineering structures, is supported on large-diameter rigid monopiles. For such structures, compared with the gravitational loads, cyclic lateral loading may often be more critical for the analysis and design. The lateral load-carrying capacity of a pile depends on its geometry (dimensions), the soil properties and type of loading. In order to increase its lateral load-carrying capacity, it is necessary either to change the properties of the near-surface layers of soil or to change its geometry. This paper presents model studies investigating a novel technique to limit the lateral deflection (rotation) of a monopile under long-term cyclic lateral loading. The technique provides enhanced restraint of the monopile through the installation of four shorter piles, arranged in a cruciform, which attach to the head of the central monopile by way of a grillage. Different aspects of this modification, including its fabrication and attachment to the monopile, are presented. Its efficiency in reducing the monopile rotation under cyclic lateral loading is evaluated through a comprehensive testing programme, with reasonably encouraging results.

## Notation

|           |  |
|-----------|--|
| $a$       | monopile rotation  |
| $b$       | rotation of monopile with piled-cruciform attachment in situ |
| $D$       | outer diameter of pile                                       |
| $d_{10}$  | effective grain size for 10% passing by mass                 |
| $d_{30}$  | effective grain size for 30% passing by mass                 |
| $d_{50}$  | mean effective grain size                                    |
| $d_{60}$  | effective grain size for 60% passing by mass                 |
| $EI$      | bending stiffness  |
| $k_h$     | initial coefficient of subgrade reaction                     |
| $L$       | monopile embedment length                                    |
| $L_{SDP}$ | embedment length of small diameter pile                      |
| $P_u$     | ultimate static lateral load-carrying capacity               |
| $\eta L$  | dimensionless embedment length of monopile                   |

## 1. Introduction

The preferred foundation solution for a particular offshore structure depends, among other factors, on the local soil

conditions, water depth, anticipated loading and financial constraints (Malhotra, 2010). Large-diameter monopiles are a frequently used foundation system for offshore wind turbines and other offshore structures. Offshore wind farms often contain can comprise many hundreds of turbines supported at heights of typically 30–80 m above mean sea level. The preferred foundation type for these tall structures in water depths of up to 30 m is large-diameter monopiles, owing to their ease of construction and installation. These monopiles are subjected to large cyclic lateral and moment loads, in addition to axial loads, as documented by LeBlanc *et al.* (2010), Bhattacharya *et al.* (2011) and Cuéllar (2011). However, their lateral load-carrying resistance may not be sufficient to withstand prolonged impact under large wind and wave loading. A solution may be achieved by simply increasing the physical dimensions of the monopile, but this may not be economically or practically feasible. Thus, a range of different foundation solutions in place of, or modifications of, the monopile are being investigated by different researchers.

Arshad, M., and O'Kelly, B.C. (2016) "Piled-cruciform attachment to monopile head reduces deflection". *Proceedings of the Institution of Civil Engineers – Geotechnical Engineering*, Volume 169, Issue Number 4, pages 321–335.  
<http://dx.doi.org/10.1680/jgeen.15.00001>

Modification of the conventional monopile by the attachment of 'wings' close to the pilehead, in order to increase the lateral load-carrying capacity and stiffness of the foundation system for weaker soil conditions (close to the mudline), has been investigated by many researchers using small-scale tests in sand under the normal gravitational ( $1g$ ) condition (Dührkop and Grabe, 2008; Nasr, 2014; Peng *et al.*, 2011) and in centrifuge facilities (Bienen *et al.*, 2012). These researchers found that, with the wings attached, the pilehead deflection substantially reduced (by  $\sim 50$ – $70\%$ ) and the ultimate lateral load-carrying capacity increased by up to  $80\%$ , depending on the length of the wings compared with the length of the monopile, the shape of the wings and the soil properties. Another alteration, comprising a monopile combined with a footing base, has also been proposed. Initial model tests performed in sand at  $1g$  were reported by Stone *et al.* (2007), with apparently promising results, suggesting that the additional rotation restraint provided by the footing can result in a stiffer lateral response and greater ultimate lateral load-carrying capacity. Arshi *et al.* (2013) performed tests in sand at  $1g$  by adding skirts of different lengths (depths) to these piled footings. Their results indicated that increasing the skirt length tends to increase the ultimate lateral load-carrying capacity of the foundation system by about  $50\%$  compared with the non-skirted hybrid system. More recently, Arshad and O'Kelly (2016b) reported  $1g$  tests in sand that investigated the use of concentric rings of small-diameter piles (SDPs) installed centrally around the model monopile. Their results showed that the rotation of the monopile, investigated under a range of cyclic lateral loading scenarios, was reduced by  $40$ – $65\%$  owing to the enhanced confinement and densification of the sand test bed provided by the presence of the SDPs.

This paper presents an experimental investigation performed to explore the possibility of pilehead modification to reduce the accumulated rotation of a monopile under long-term cyclic lateral loading. The novel solution proposed comprises four shorter SDPs, arranged in a cruciform, which attach by way of a grillage to the pilehead at the mudline level. From a review of the literature, this would appear to be the first study of its kind in relation to the proposed set-up for deep foundation structures. On the basis of encouraging results, it can be expected that this novel technique may prove to be a viable solution to enhance the serviceable life of structures supported by monopiles that are subjected to long-term cyclic lateral loading, such as offshore wind-turbine structures (OWTs).

## 2. Development of the proposed arrangement

### 2.1 Governing loading for OWT monopile foundation system

Monopile foundations for offshore wind-turbine structures are typically manufactured from steel tubular sections with an outer diameter ( $D$ ) of up to  $7.5$  m, wall thicknesses of up to  $150$  mm and embedment depths of between  $15$  and  $30$  m

(Achmus *et al.*, 2009). Monopile foundations are generally used in shallow water depths (i.e. typically  $< 30$  m), generally becoming too flexible for water depths of between  $\sim 30$  and  $40$  m, in which case monopiles fitted with guy wires or tripod solutions are considered as economical alternatives. For greater water depths ( $> 40$  m), time-consuming installation and the effects of soil degradation ('potholing') that occurs in-service at mudline level around the pile make monopile foundations prohibitive (Irvine *et al.*, 2003). Other foundation options, as discussed by Arshad and O'Kelly (2013, 2016a) and O'Kelly and Arshad (2016), are then considered to be viable. The serviceability limit state is largely determined by the lateral deflection (rotation) response of the monopile under many millions of load cycles; for example, over the service life of a  $2$  MW OWT structure,  $10^7$  lateral load cycles of  $1.4$  MN magnitude (corresponding to the fatigue loading for design) are expected to occur (Germanischer Lloyd, 2005).

The monopile must mobilise sufficient soil resistance over its embedded length to transfer all types of applied loads to the surrounding soil, with adequate safety factors, and prevent toe 'kick' (displacement of the pile base) and excessive deflection/rotation of the pile itself. According to current practice, monopiles are analysed for the axial loads only to determine their bearing capacity and settlement responses, and then for the lateral loads only to determine their lateral load-carrying capacity and flexural behaviour (Karthigeeyan *et al.*, 2006; Moayed *et al.*, 2012). Compared with the axial loads, the lateral loads are considered to be governing, as mentioned in several design guidelines (API, 2010; DNV, 2011; Germanischer Lloyd, 2005) and documented by many researchers (Achmus, 2010; Bhattacharya *et al.*, 2013; Carswell *et al.*, 2015; Haiderali *et al.*, 2013; Kuo *et al.*, 2012; Leblanc *et al.*, 2010; Lombardi *et al.*, 2013; Malhotra, 2010; Nicolai and Ibsen, 2014; Peng *et al.*, 2011; Zhu *et al.*, 2013). In other words, the required diameter, wall thickness and embedment length of the monopile is generally dictated by the applied lateral loads and moments. Hence, the experimental work presented in this paper focuses on the enhancement of the lateral stability of the conventional monopile, with a novel modification to the pilehead proposed, namely four SDPs arranged in a cruciform that attach by way of a grillage to the pilehead.

### 2.2 Geometric details of proposed arrangement

Figure 1 shows a schematic diagram of the proposed arrangement at reduced scale, which consists of a central 'split-able' ring with four radial steel arms, each fitted with a smaller diameter ring (sleeve ring) at its far end. The two halves of the central ring, manufactured from  $30$  mm wide  $\times$   $2$  mm thick steel strip, are secured together by way of their collars, using M4 nut-bolts, clamping around the head of the monopile ( $D = 53$  mm). Four radial struts welded to the central ring, each having length, width and thickness dimensions of  $85$ ,  $20$  and  $2$  mm, respectively, were arranged in a cruciform, making the four arms. The far end of each of these arms was

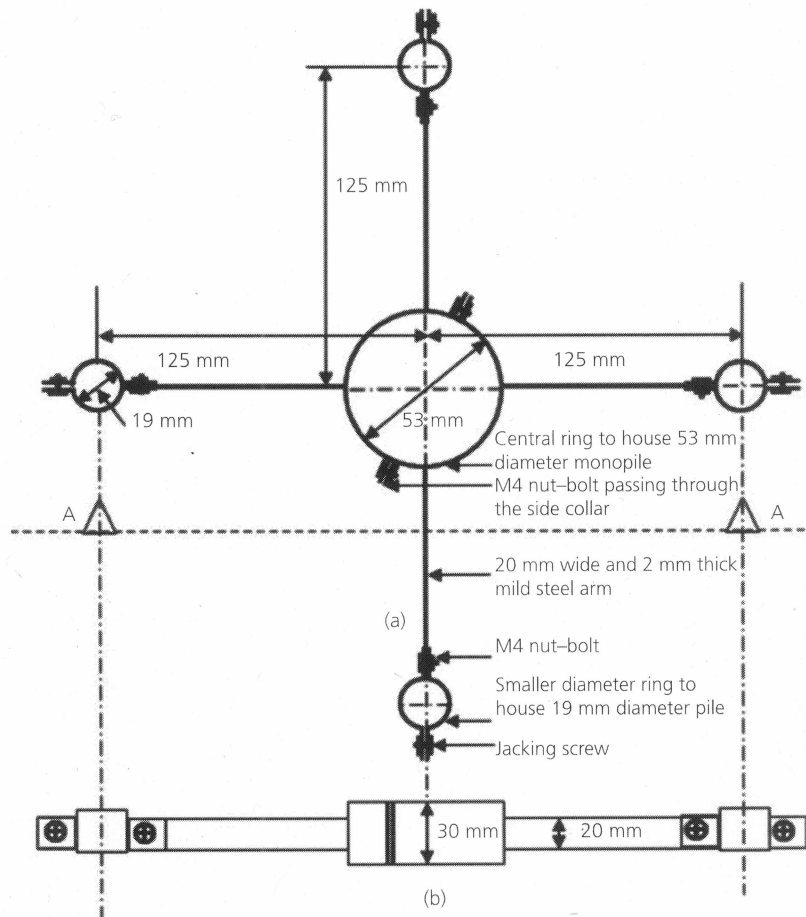


Figure 1. Schematic diagram of cruciform attachment for monopile: (a) plan view; (b) side view (section A–A)

connected by an M4 nut–bolt to a sleeve ring, manufactured from 25 mm wide  $\times$  2 mm thick steel strip. The connections between the radial arms and sleeve rings allowed changes to be made to the inclination of the SDPs that were housed in these rings. The sleeve rings were equipped with jacking screws (see Figure 1) that allowed the required adjustments to be made to the solid SDPs ( $D=19$  mm; i.e. 36% of the monopile diameter) during their installation in the sand beds (described later).

Figure 2 shows the arrangement centred on the monopile, with the four solid SDPs aligned vertically and attached by way of the grillage to the pilehead. Hereafter, the central split-able ring (holding the monopile) and the four radial arms holding the SDPs are collectively termed as the piled-cruciform arrangement.

### 2.3 Working mechanism of piled-cruciform arrangement

The soil around the monopile is influenced by the cyclic lateral loading (Bhattacharya and Adhikari, 2011; Bhattacharya

*et al.*, 2011; Cuéllar *et al.*, 2012; LeBlanc *et al.*, 2010; Rosquoët *et al.*, 2007). For sandy soil, it can be argued that the zone of significant influence remains limited to within 2–3 $D$  measured from the monopile axis, as evident from the formation of a cone of depression observed at the sand bed surface level around the monopile during 1 $g$  testing (Brown *et al.*, 1988; Cuéllar *et al.*, 2012). For lateral loading, the upper part of the soil deposit around the monopile is more critical than the lower part, owing to the greater level of deflection occurring closer to the pilehead (Nasr, 2014; Zhang *et al.*, 2005).

Conceptually, the piled-cruciform attachment is designed to transfer some of the applied lateral load away from the zone of significant influence for the monopile. Under the action of the applied lateral loading/moment, the monopile and piled-cruciform attachment tend to deflect (rotate with respect to their initial vertical alignment), with resistance provided by the passive pressures (forces) mobilised along the embedded lengths of the monopile and four SDPs (the latter are transmitted by way of the cruciform arms to the pilehead). Through this arrangement, the stress intensity is reduced in the

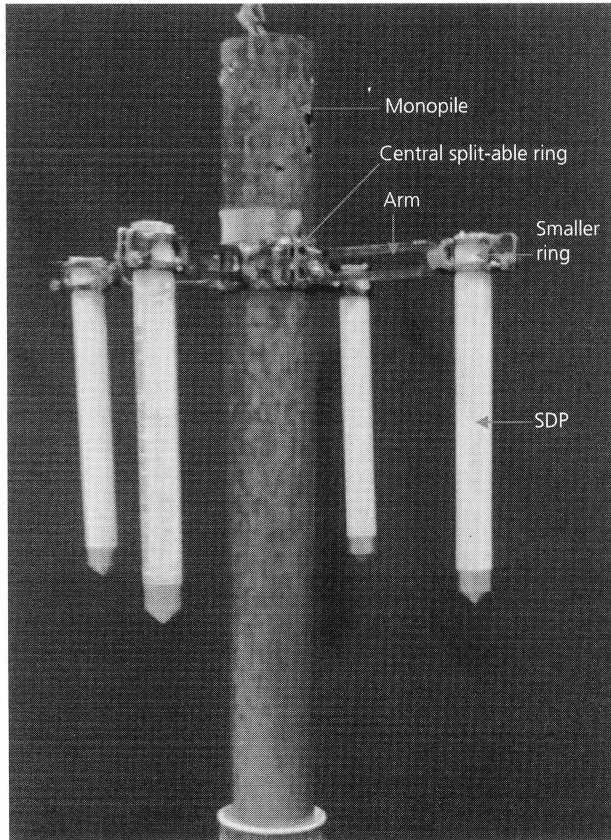


Figure 2. Piled-cruciform arrangement attached to monopile

immediate vicinity of the monopile, thereby lowering the strain developed in the surrounding soil, as compared with the monopile alone for the same magnitude of lateral load. Further, instead of having a 'free' pilehead, the rotation is restrained by the cruciform arm attachment. The proposed set-up also produces a significant increase in the bending stiffness, as compared with the conventional monopile. For instance, considering the structural elements in the present experimental set-up, the second moment of area about the centroidal axis of the 53 mm diameter hollow monopile was  $4.5 \times 10^4 \text{ mm}^4$ , with its value increased to  $\sim 8.9 \times 10^6 \text{ mm}^4$  at the mudline level when fitted with the piled-cruciform attachment; that is, 200 times greater.

### 3. Testing facility, instrumentation and model pile

For the present study, the Trinity College Dublin electro-mechanical loading system for testing model piles at 1g (Figure 3) was used. This system is capable of applying many thousands of lateral load cycles on scaled models, with full control provided over the loading direction, amplitude, frequency and waveform shape. Further details on its working mechanism and capabilities, including the instrumentation used to measure the lateral loads applied to the pilehead and

the resulting axial and lateral deflections and rotation response of the pile (Figure 4) are presented in the paper by Arshad and O'Kelly (2014).

The model pile was manufactured from smooth brass tubing, having an overall length of 540 mm, outer diameter of 53.0 mm and wall thickness of 0.8 mm, which produced a bending stiffness ( $EI$ ) value of  $4.33 \text{ kN m}^2$ . Its lower end was closed using a 3 mm thick brass plate in order to represent a fully plugged tubular pile. Geometrically, the pile set-up, with an embedded length ( $L$ ) to outer diameter ( $D$ ) ratio of 6.8 at the start of each loading test performed, is categorised as a short 'rigid' pile, which encompasses  $L/D$  ratios of up to 10 (DNV, 2011; Peng *et al.*, 2011; Tomlinson, 2001). To verify this, the pile's rigidity was evaluated based on its value of the dimensionless embedment length,  $\eta L$  (Broms, 1964). The coefficient  $\eta$  is calculated as

$$1. \quad \eta = \left( \frac{k_h}{EI} \right)^{1/5}$$

where  $k_h$  is the initial coefficient of subgrade reaction and  $EI$  is the bending stiffness of the monopile.

According to Terzaghi (1955), the value of  $k_h$  is  $19.8 \text{ MN/m}^3$  for dense sand (which was the soil investigated in the present study). A pile is considered to be a short rigid pile for  $\eta L < 2$  and a long elastic pile for  $\eta L > 4$  (Broms, 1964; Chari and Meyerhof, 1983). The estimated  $\eta L$  value of 1.94 for the monopile set-up in the present investigation indicates that the model pile satisfied the criterion for short rigid piles.

The model pile was partially embedded in dense sand beds prepared in a 0.95 m dia. by 0.6 m deep steel tank. These dimensions were chosen to ensure that for the static and cyclic lateral loading scenarios investigated in the present study, the failure wedge for the pile would not extend to the tank boundaries. With a ratio of tank diameter to pile diameter of almost 18, side wall boundary effects were not considered to be significant (Davie and Sutherland, 1978; Rao *et al.*, 1996). Similarly, a soil cushion (sand in the present case) having a thickness of  $3-4D$  located below the pile base was considered sufficient to absorb the small vertical stress field (LeBlanc *et al.*, 2010).

### 4. Sand characterisation and sand bed preparation, including monopile and SDP installation

All of the tests performed used commercially available air-dried Glenview sand, comprising sub-angular to angular grains ranging from 0.1 to 1.0 mm in size, with  $d_{10}$ ,  $d_{30}$ ,  $d_{50}$  and  $d_{60}$  values of 0.16, 0.22, 0.27 and 0.31 mm, respectively, giving a coefficient of uniformity value of 1.94 and coefficient of curvature value of 0.98. Furthermore, the sand had minimum and maximum dry density values of 1388 and

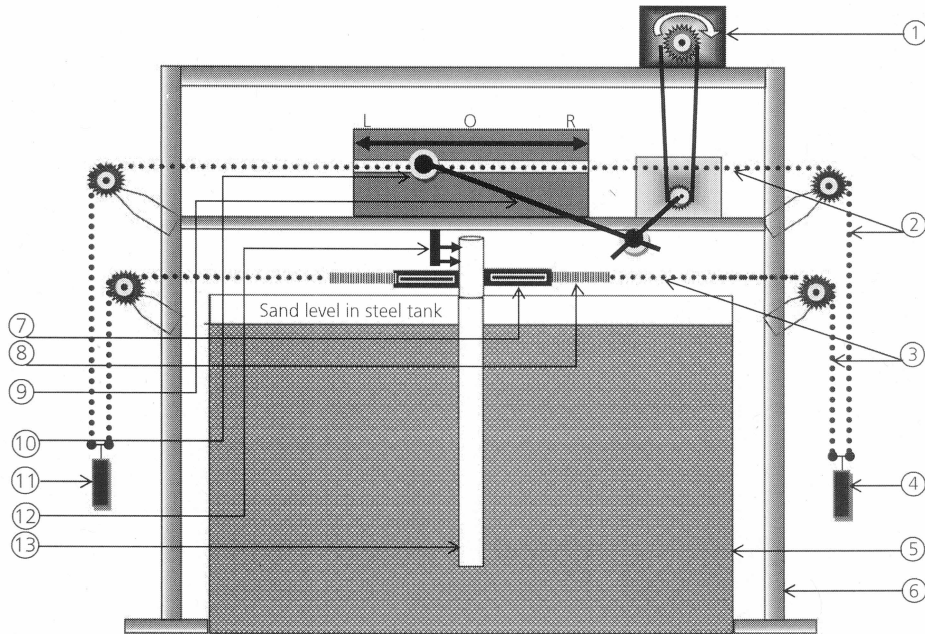


**Figure 3.** Schematic diagram of the experimental rig for model pile studies, set up for two-way lateral loading of the pilehead. Note: 1, drive motor; 2, upper right chain segment; 3, lower right chain segment; 4, right loading hanger, with weight; 5, steel tank; 6, reaction frame; 7, right load cell; 8, right spring; 9,

articulated arm; 10, sliding node; 11, left loading hanger, with weight; 12, reference support with two horizontal displacement transducers; 13, monopile, shown without piled-cruciform attachment (adopted from Arshad and O'Kelly (2014))

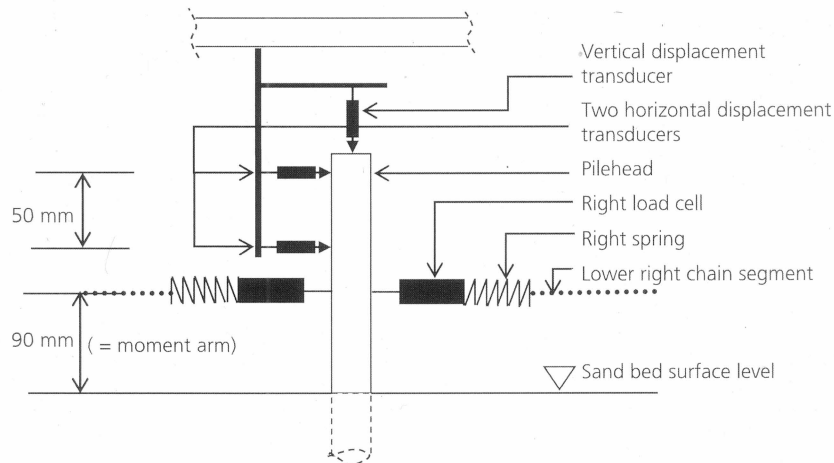


**Figure 4.** Arrangement of load cells and displacement transducers at the pilehead (adopted from Arshad and O'Kelly (2014))

1662 kg/m<sup>3</sup>, respectively, equating to maximum and minimum void ratio values of 0.92 and 0.60, respectively. At maximum density, the dry sand had a peak friction angle of 39°, determined using 60 mm-square shearbox tests.

The sand was air-pluviated into the steel tank, gently raining in six separate layers, each 100 kg in mass. This produced approximately 90 mm thick deposited layers. After the first two layers of sand had been deposited in the tank, the model

pile was positioned vertically at the centre of the tank, with temporary support to its head provided by four tensioned horizontal steel wires that were secured radially from the wall of the tank. Four more layers of sand were then deposited, bringing the sand bed to its full depth of 0.54 m (i.e. pile embedment length of 0.36 m). During this process, the surface of the deposited sand layer was levelled, as necessary, using a straight edge before depositing the next sand layer. For all of the sand beds prepared in the present investigation, this preparation technique was found to produce sand beds having a dry density of  $1577 \pm 6 \text{ kg/m}^3$  (density index range of 70–74%). The resulting 'wished in place' pile simulated a pre-bored pile; in other words, no displacement would occur in the sand deposit as a result of the pile installation.

On completion of the sand bed with pile installed, the split-able ring attachment was clamped around the pilehead such that its cruciform arms were located just above the finished sand surface level in the steel tank. In the next step, four SDPs were inserted through the sleeve rings and pushed into the sand bed to the required embedment depth (Figure 5). Jacking screws on the sleeve rings (see Figure 1) allowed some fine adjustments before rigidly connecting them to the heads of the SDPs.

## 5. Testing programme

A comprehensive programme of cyclic lateral loading tests (see Table 1) was performed on the model pile in the dense sand beds to evaluate the efficiency of the proposed arrangement. The tests investigated a load amplitude of 60 N, two loading frequencies of 0.25 and 0.4 Hz, and different loading directions (one-way, partial one-way, balanced and unbalanced

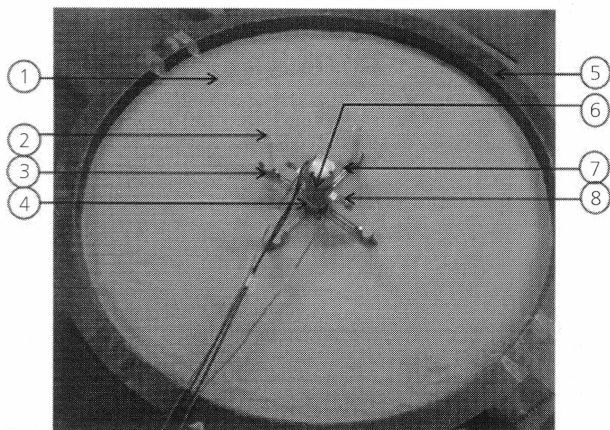


**Figure 5.** Piled-cruciform arrangement attached to head of monopile installed in dry sand bed. Note: 1, sand bed surface; 2, protruding head of SDP; 3, sleeve ring; 4, central 'split-able' ring; 5, steel tank perimeter; 6, protruding head of central monopile; 7, cruciform arm; 8, miniature load cell attached to pile shaft at a distance of 90 mm above the sand bed surface level

| Test number | Set-up<br>(refer to Table 2) | Loading scenario<br>(test ID) |
|-------------|------------------------------|-------------------------------|
| 1           | Reference                    | 2w/30–60/0.4                  |
| 2           | A                            | 2w/30–60/0.4/A                |
| 3           | B                            | 2w/30–60/0.4/B                |
| 4           | C                            | 2w/30–60/0.4/C                |
| 5           | D                            | 2w/30–60/0.4/D                |
| 6           | E                            | 2w/30–60/0.4/E                |
| 7           | Reference                    | 2w/60–60/0.4                  |
| 8           | A                            | 2w/60–60/0.4/A                |
| 9           | B                            | 2w/60–60/0.4/B                |
| 10          | C                            | 2w/60–60/0.4/C                |
| 11          | D                            | 2w/60–60/0.4/D                |
| 12          | Reference                    | 1w/60/0.25                    |
| 13          | A                            | 1w/60/0.25/A                  |
| 14          | B                            | 1w/60/0.25/B                  |
| 15          | C                            | 1w/60/0.25/C                  |
| 16          | Reference                    | 1w/30–60/0.25                 |
| 17          | A                            | 1w/30–60/0.25/A               |
| 18          | B                            | 1w/30–60/0.25/B               |

**Table 1.** Cyclic lateral loading test programme

two-way loading conditions), with typically 12 000 lateral load cycles applied during each test. For one-way loading, the applied load ranged between zero and some maximum load value, whereas for partial one-way loading, the applied load ranged between some value above zero and the maximum load value. With respect to the ultimate static lateral load-carrying capacity ( $P_u$ ) of the pile, the load amplitude of 60 N corresponds to its serviceability limit state ( $\sim 42\%$  of  $P_u$  (DNV, 2011)).

The tests performed are identified as follows: lateral loading direction (1w, one-way; 2w, two-way)/load amplitude (N)/frequency (Hz). For instance, 1w/60/0.25 indicates one-way lateral loading of the monopile (without the piled-cruciform arrangement in situ) for an amplitude of 60 N and frequency of 0.25 Hz. 1w/30–60/0.25 indicates one-way lateral loading, with the load fluctuating from 30 to 60 N from the same side at 0.25 Hz. 2w/30–60/0.4 indicates unbalanced two-way lateral loading, 30 N in one direction and 60 N in the other, applied at a frequency of 0.4 Hz.

Table 2 shows the different formations of the piled-cruciform arrangement investigated (labelled set-ups A–E), namely: (a) ratio of embedment length of the SDPs ( $L_{SDP}$ ) to that of the monopile ( $L$ ); (b) inclination of the SDPs from the vertical direction; (c) orientation of the cruciform grillage with respect to the line of action of the applied loading. For all of the static and cyclic tests performed, the lateral loading was applied to the side of the model pile at an elevation of 90 mm above the sand bed surface level.

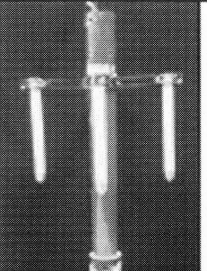
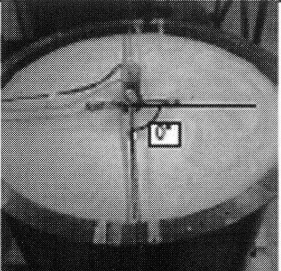
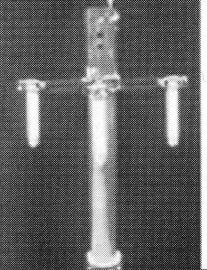
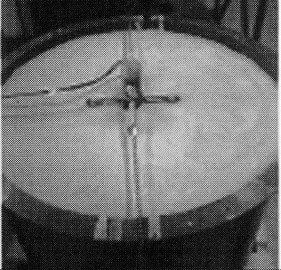
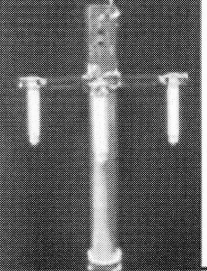
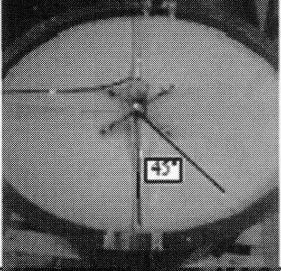
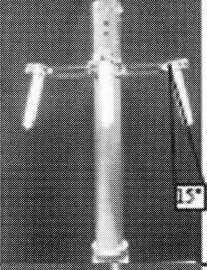
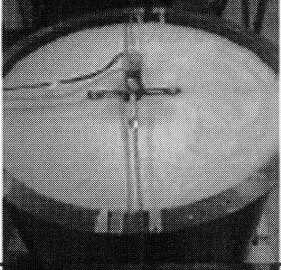
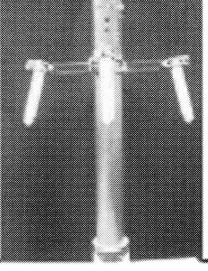
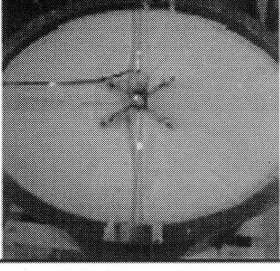
| Set-up | SDP length ( $L_{SDP}$ ) and inclination to vertical direction                      | Offset of cruciform arms with respect to line of action of applied loading          | Comment   |
|--------|---|---|---|
| A      |    |    | Cruciform arms are aligned with the line of action of the cyclic lateral loading.<br><br>Vertical SDPs are half the length of the central monopile ( $L$ ) – that is, $L_{SDP}/L = 0.5$ . |
| B      |   |   | As per set-up A, apart from the SDPs being one-third of the monopile length – that is, $L_{SDP}/L = 0.33$ .   |
| C      |  |  | Cruciform arms are offset by $45^\circ$ from the line of action of the cyclic lateral loading.<br><br>Vertical SDPs are one-third of the monopile length; that is, $L_{SDP}/L = 0.33$ .   |
| D      |  |  | As per set-up B, apart from the SDPs being inclined at $15^\circ$ to the vertical direction.  |
| E      |  |  | As per set-up C, apart from the SDPs being inclined at $15^\circ$ to the vertical direction.  |

Table 2. Different set-ups of the piled-cruciform attachment investigated

## 6. Ultimate static lateral load-carrying capacity of monopile

Static lateral loads were applied in small increments of 10 N to the model pile in order to evaluate its ultimate static lateral load-carrying capacity, with and without the piled-cruciform attachment in situ. The lateral deflection response of the pilehead was monitored using two horizontally mounted displacement transducers (Figure 4), with the transducer readings allowed to stabilise before the application of the next load increment. The rotation response of the rigid pile was calculated using these displacement measurements, as described in the paper by Arshad and O'Kelly (2014).

Different assumptions have been used by researchers regarding the determination of the ultimate static lateral load-carrying capacity, although they are generally based on excessive lateral displacement of the pilehead or rotation of the pile (Hu *et al.*, 2006; Nasr, 2014; Peng *et al.*, 2011). Some researchers determine the value of  $P_u$  as corresponding to a point on the load-deflection (rotation) curve where the pile starts to deflect (rotate) significantly for a relatively small increase in the lateral load (Dickin and Laman, 2003; Prasad and Chari, 1999).

Figure 6 shows the static lateral load-rotation relationships obtained for monopiles having five different piled-cruciform arrangements (set-ups A-E in Table 2) investigated as part of the present study, along with reference data for the monopile alone. Previous studies of rigid, model pile behaviour performed at 1g usually estimated the  $P_u$  value for lateral pile deflections of  $0.1-0.2 \times D$  (Cuéllar *et al.*, 2012; El Sawwaf,

2006; Peng *et al.*, 2011; Uncuoğlu and Laman, 2011) occurring at the sand bed surface level. Hence, in the present investigation, the value of  $P_u$  for the reference monopile was estimated as 140 N, which corresponded to a point on its experimental load-rotation curve (Figure 6) where, apparently, the surrounding sand began to yield substantially; that is, its rotation increased by  $0.4^\circ$  over the load increment from 120 to 140 N, whereas it increased by almost  $1.0^\circ$  for the load increment from 140 to 160 N. For this point (140 N), the model pile had rotated by  $1.5^\circ$  from its initial vertical alignment, producing a lateral deflection (measured at the sand bed surface level) of  $\sim 7$  mm; that is,  $0.13 \times D$ . From Figure 6, it can be interpreted that the inclusion of the different piled-cruciform arrangements all substantially improved the ultimate static lateral load-carrying capacity of the monopile, as summarised in Table 3 for quick comparison.

## 7. Performance of piled-cruciform arrangement in reducing monopile rotation under cyclic lateral loading

### 7.1 Effect of SDP embedment length

Twelve tests were performed to investigate the effect of the SDP embedment length on the rotation response of the monopile, considering four different loading scenarios and two  $L_{SDP}/L$  values of 0.5 and 0.33 (set-ups A and B, respectively, in Table 2). Figures 7(a) and 7(b) show the rotation responses of the monopile for one-way and partial one-way loading, respectively, while Figures 7(c) and 7(d) show its responses for balanced and unbalanced two-way loading, respectively.

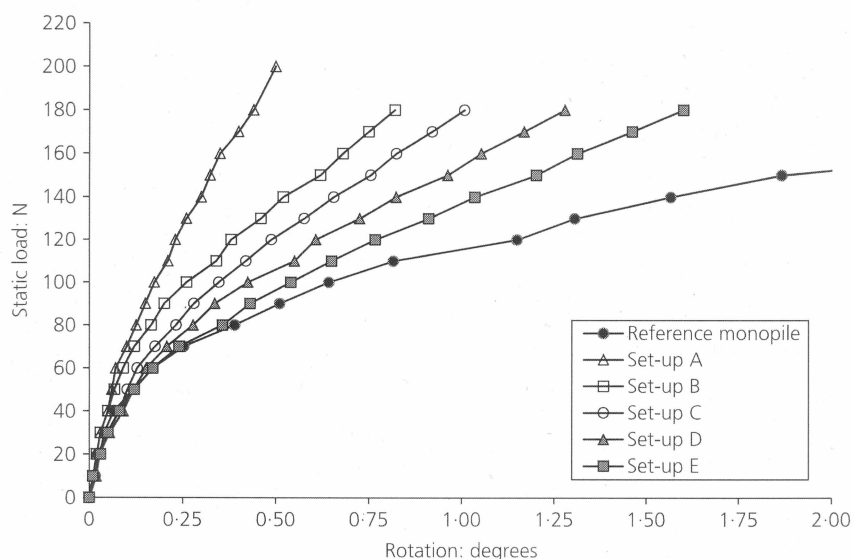


Figure 6. Static lateral load plotted against rotation relationships for the different experimental set-ups shown in Table 2



| Set-up<br>(refer to Table 2) | Lateral<br>resistance: N | Rotation:<br>degrees |
|------------------------------|--------------------------|----------------------|
| Reference                    | 90                       | 0.5                  |
| A                            | 200                      | 0.5                  |
| B                            | 136                      | 0.5                  |
| C                            | 122                      | 0.5                  |
| D                            | 106                      | 0.5                  |
| E                            | 96                       | 0.5                  |
| Reference                    | 150                      | 1.88                 |
| A                            | 150                      | 0.32                 |
| B                            | 150                      | 0.62                 |
| C                            | 150                      | 0.76                 |
| D                            | 150                      | 0.96                 |
| E                            | 150                      | 1.2                  |

**Table 3.** Lateral resistance mobilised for 0.5° rotation of monopile, and monopile rotation produced by an applied lateral load of 150 N, for the different set-ups of the piled-cruciform attachment

From these figures, it can be interpreted that the piled-cruciform attachment to the monopile considerably reduced its accumulated rotation, when compared with the reference monopile for the same loading condition. For instance, at 6000 load cycles for the unbalanced two-way loading scenario of 2w/30-60/0.40 (Figure 7(d)), the reference monopile had rotated by 2.75°, whereas with the piled-cruciform attachment in situ, its rotation was limited to 0.49° and 0.38° for  $L_{SDP}/L$  values of 0.33 and 0.5, respectively; that is, 82% and 86% reductions in the monopile rotation were achieved (as determined using Equation 2). The respective reductions in the monopile rotation were 57% and 68% for balanced two-way loading (i.e. 2w/60-60/0.40 in Figure 7(c)), and 24% and 31% for one-way loading (i.e. 1w/60/0.25 in Figure 7(a)). For partial one-way loading (i.e. 1w/30-60/0.25 in Figure 7(b)), when compared with the reference monopile, the rotation was found to reduce by 73% for both  $L_{SDP}/L$  values investigated. The reduction in the monopile rotation can be largely explained by the additional passive resistances mobilised along the

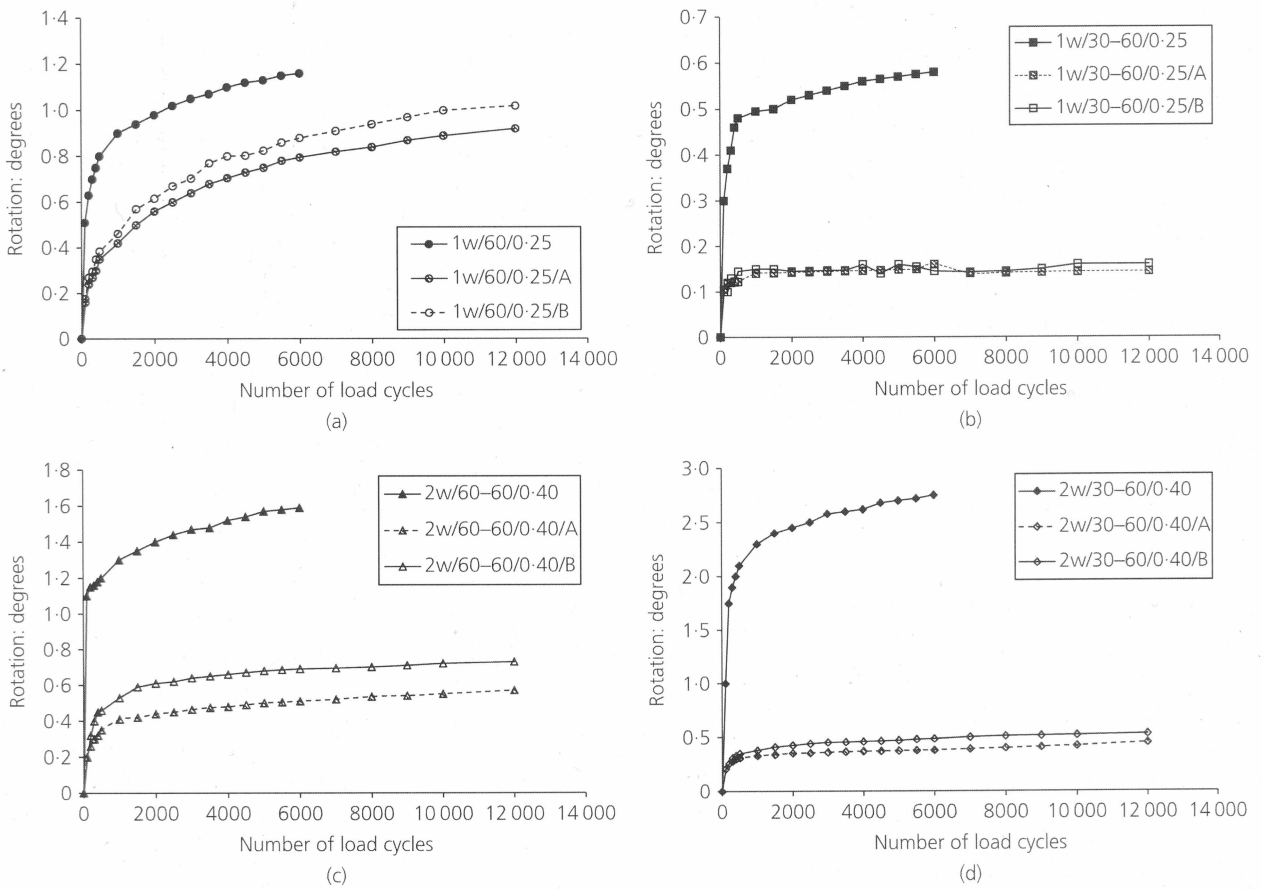


**Figure 7.** Effect of SDP embedment length on accumulated rotation of the monopile: (a) one-way loading; (b) partial one-way loading; (c) balanced two-way loading (d) unbalanced two-way loading

Arshad, M., and O'Kelly, B.C. (2016) "Piled-cruciform attachment to monopile head reduces deflection". *Proceedings of the Institution of Civil Engineers – Geotechnical Engineering*, Volume 169, Issue Number 4, pages 321–335.  
<http://dx.doi.org/10.1680/jgeen.15.00001>

embedded lengths of the four SDPs, as described in Section 2.

$$2. \text{ Reduction (as \%)} = \left( \frac{a-b}{a} \right) \times 100$$

where  $a$  is the monopile rotation and  $b$  is the rotation of the monopile with the piled-cruciform attachment in situ.

Figure 8 shows the percentage reduction in the monopile rotation produced when the  $L_{SDP}/L$  ratio was increased from 0.33 to 0.5. From this figure, it can be concluded that, for this 50% increase in the  $L_{SDP}/L$  value, the monopile rotation was reduced by between 9% and 27% over the 12 000 load cycles applied. Hence, for practical purposes, based on these model test results, there is no major benefit achieved in increasing the  $L_{SDP}/L$  ratio from 0.33 to 0.5.

### 7.2 Effect of loading direction orientation

Six of the tests performed were designed to investigate two different orientations of the piled-cruciform arrangement, with respect to the line of action of the applied loading (set-ups B and C in Table 2), considering three different loading scenarios and an  $L_{SDP}/L$  value of 0.33. Figure 9 shows that relatively greater rotation of the monopile occurred when the cruciform arms were offset by 45° from the line of action of the applied loading (set-up C), as compared with full alignment (set-up B), although the difference was marginal for the one-way and balanced two-way loading scenarios investigated. For instance, at 6000 load cycles, the monopile had rotated by 0.92° (1w/60/0.25/C in Figure 9(a)) and 0.73° (2w/60–60/0.40/C in Figure 9(b)) for set-up C, compared with 0.88° and 0.69°, respectively, for set-up B. However, the effect was significant for unbalanced two-way loading (2w/30–60/0.4 in Figure 9(c)), with monopile rotations of 0.76° and 0.49° measured for set-ups C and B, respectively, at 6000 load cycles. A possible reason for the greater rotation experienced for set-up C may be the decrease in perpendicular distance (from

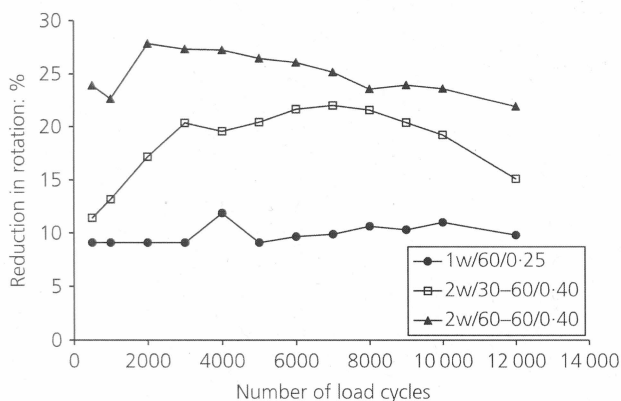


Figure 8. Percentage reduction in accumulated rotation of monopile achieved by increasing  $L_{SDP}/L$  value from 0.33 to 0.5

125.0 to 88.4 mm) between the SDP centres and the axis of the monopile orthogonal to the loading direction (see Figure 10), which may have the effect of causing some greater overlap between the zones of significant influence for the laterally loaded

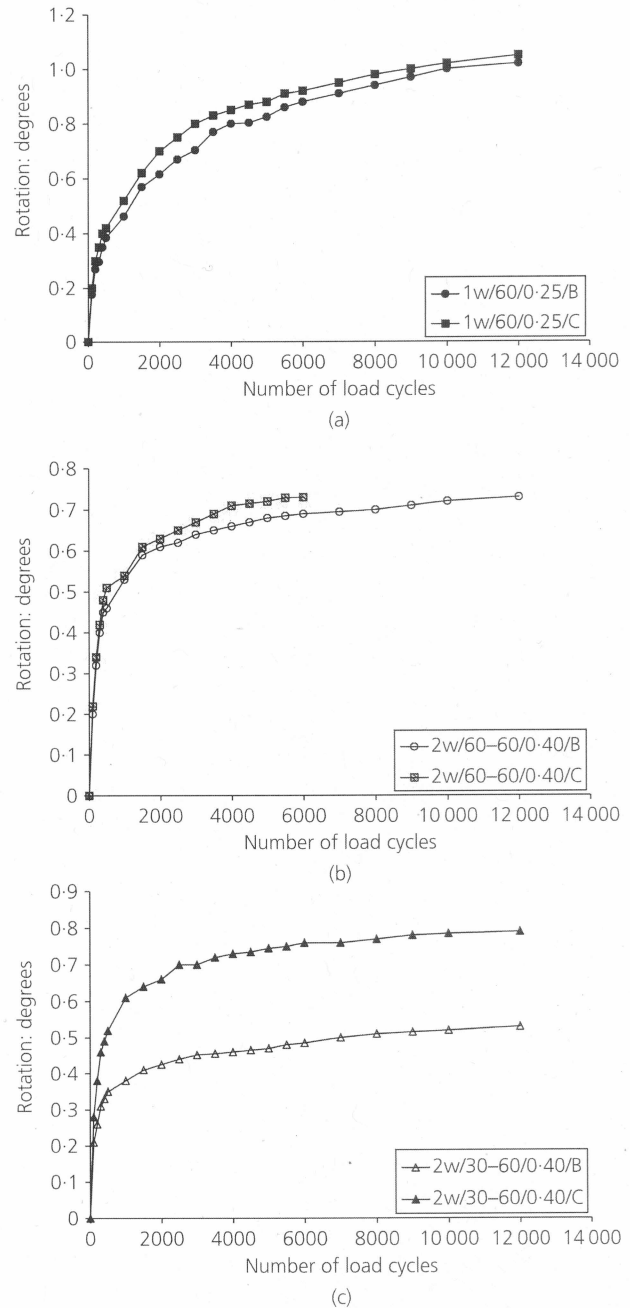
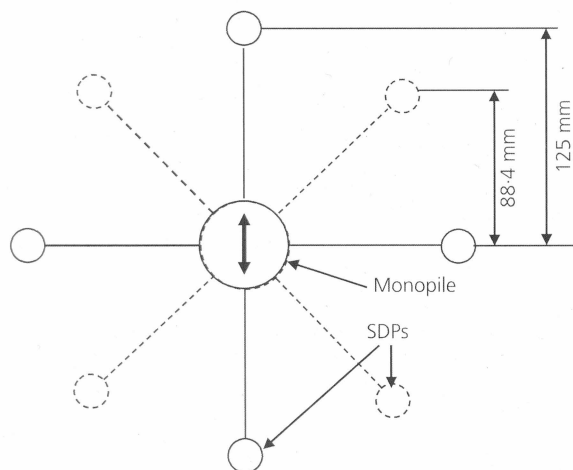


Figure 9. Effect of orientation of piled-cruciform attachment, with respect to line of action of the applied loading, on accumulated rotation of monopile: (a) one-way loading; (b) balanced two-way loading; (c) unbalanced two-way loading



**Figure 10.** Relative positions of SDPs when the cruciform arms were aligned with, and offset by 45° from, the line of action of the applied loading

monopile and SDPs. For practical reasons, it can be considered that the more favourable orientation occurs for the cruciform arms aligned with the line of action of the applied loading.

### 7.3 Effect of SDP inclination

The efficiency of the piled-cruciform arrangement was also evaluated for different inclinations (to the vertical direction) of the SDPs at an  $L_{SDP}/L$  value of 0.33. For this purpose, the four SDPs were inclined outward, at 15° to the vertical direction, and the monopile tested under balanced and unbalanced two-way loading, with the cruciform arms aligned with the line of action of the applied loading (set-up D in Table 2). Figures 11(a) and 11(b) show the effect of this change in inclination, comparing set-up D with set-up B (see Table 2). From these figures, it can be concluded that, for both of these loading scenarios investigated, the set-up with the inclined SDPs produced greater monopile rotation. For instance, compared with the vertical SDPs (set-up B), the monopile rotation for the SDPs inclined at 15° under balanced two-way loading (2w/60–60/0.4/D in Figure 11(a)) was 5–9% greater between the 1000th and 6000th load cycles. For unbalanced two-way loading (2w/30–60/0.4/D in Figure 11(b)), the corresponding increase was in the range 16–25% (the same percentage range increase also occurring for up to the maximum number of load cycles of 12 000 applied).

Another test was performed for unbalanced two-way loading, with the SDPs inclined at 15°, but with the cruciform arms offset by 45° from the line of action of the applied loading (set-up E in Table 2). Compared with set-up B (i.e. cruciform arms aligned with the lateral loading direction), the monopile rotation for this arrangement (2w/30–60/0.4/E in Figure 11(b)) was 97% greater at the 1000th load cycle, reducing to 74% at the 12 000th load cycle.

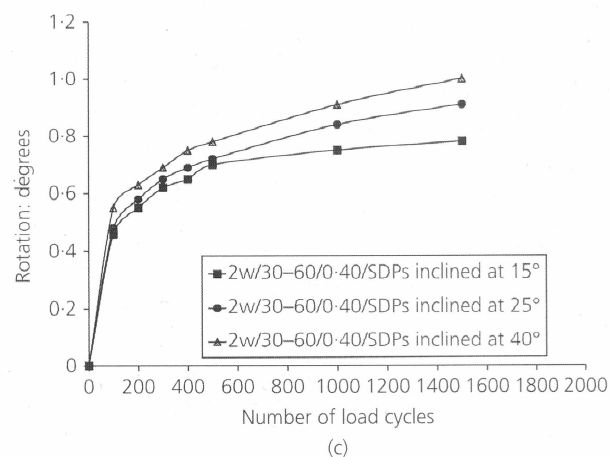
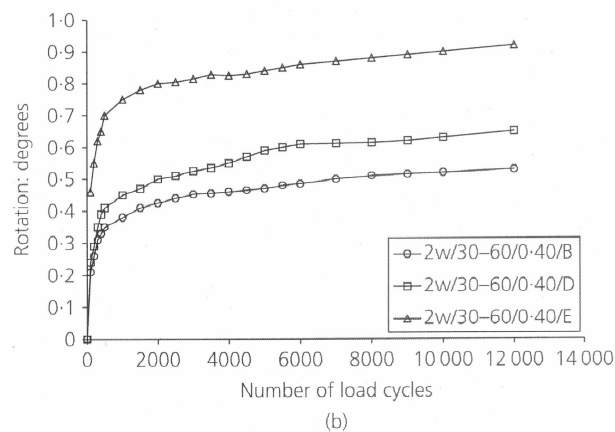
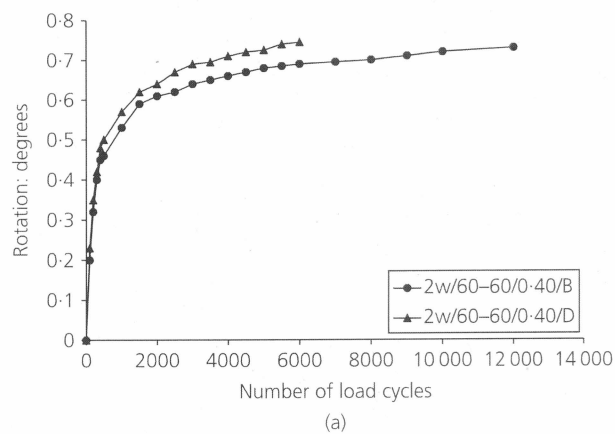


**Figure 11.** Effect of SDP inclination to vertical direction on accumulated rotation of monopile: (a) 15°, balanced two-way loading; (b) 15°, unbalanced two-way loading; (c) 15°, 25° and 40°, unbalanced two-way loading

A possible reason for the increase in monopile rotation for the inclined SDPs may be their lower resistance against the pulling action of the applied lateral loading, which is certainly greater for vertical SDPs. This hypothesis was investigated by

performing some additional tests, each involving 1500 cycles of unbalanced two-way lateral loading (2w/30–60/0.4), for the same  $L_{SDP}/L$  value of 0.33, with the cruciform arms in line with the loading direction, but setting the inclination of the SDPs at 15°, 25° and 40° to the vertical direction (Figure 11(c)). At the 1500th load cycle, the monopile rotation values for the 25° and 40° settings were found to be 17% and 28% greater compared with the 15° setting. It is the authors' view that it is probable this situation could be reversed if these SDPs were replaced by helical piles of similar dimensions.

### 8. Effect of piled-cruciform on cyclic stiffness of soil-pile system

The cyclic stiffness of the soil-pile system was calculated and plotted in Figure 12 for the series of tests reported in Tables 1 and 2. The overall trend in the variation of cyclic stiffness with increasing number of load cycles was broadly similar for set-ups with and without the piled-cruciform attached to the monopile. For a given set-up, a marginal overall increase in cyclic stiffness occurred for one-way loading (Figure 12(a)); for example, compared with the reference monopile (1w/60/0.25), the values of cyclic stiffness mobilised with the piled-cruciform attachment in situ (set-ups B and C) were typically 20–30% greater over the 1000–6000 load cycle range. For partial one-way loading (1w/30–60/0.25 in Figure 12(a)), the increase in cyclic stiffness was significantly greater (typically 70–130% over the same load cycle range for set-ups A and B).

For balanced two-way loading with the piled-cruciform attachment in situ (set-ups A–C in Figure 12(b)), the values of cyclic stiffness increased from ~230 N/mm to 380 N/mm over the 1000–6000 load cycle range (and to 450 N/mm at 10 000 load cycles), whereas the reference data increased from ~170 to 265 N/mm over the same range. For unbalanced two-way loading over the 1000–6000 load cycle range, with the piled-cruciform attachment in situ (considering set-ups A–C in Figure 12(c)), the cyclic stiffness increased from ~350 to 415 N/mm, compared with ~195 to 310 N/mm for the reference data (2w/30–60/0.4). Comparing the responses for set-ups A and B, it was found that the initial values and rates of increase in cyclic stiffness were marginally greater for set-up A, which can be explained by its greater  $L_{SDP}/L$  value of 0.5 (compared with 0.33 for set-up B), although overall, the difference was not great. This is consistent with the earlier finding that there was no major benefit (in terms of the reduction in monopile rotation) achieved in increasing the  $L_{SDP}/L$  ratio from 0.33 to 0.5 (see Figures 7 and 8).

Achmus *et al.* (2009), API (2010) and DNV (2011) have suggested that, irrespective of soil type, the stiffness of the soil-pile system degrades under cyclic lateral loading. In contrast, Rosquoët *et al.* (2007), LeBlanc *et al.* (2010), Bhattacharya *et al.* (2011) and Cuéllar *et al.* (2012) have reported that the foundation stiffness actually increases with the number of lateral load cycles, on account of densification of the sandy

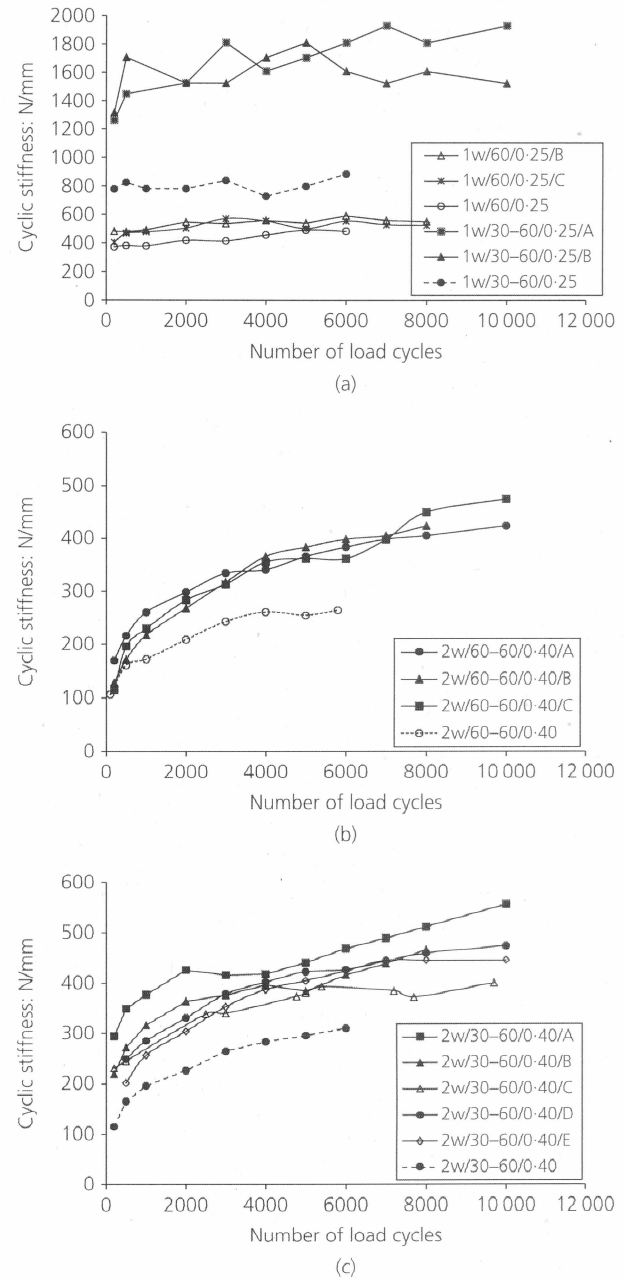


Figure 12. Cyclic stiffness response of the different foundation set-ups: (a) one-way loading; (b) balanced two-way loading; (c) unbalanced two-way loading

soil next to the monopile. The present experimental findings also indicate an increase in foundation stiffness with increasing number of lateral load cycles.

The change in stiffness of the soil-pile system with increasing number of load cycles may adversely affect the performance of the structure supported by the monopile. For instance, an

increase in cyclic stiffness of the foundation system would increase its natural frequency of vibration, which could potentially lead to resonance occurring when the forcing frequency and the natural vibration frequency of the system come close to one another. This would cause increased deflection (rotation) of the monopile, which in turn may cause more rapid deterioration of the on-board machinery and, in some cases, may ultimately lead to structural failure (Adhikari and Bhattacharya, 2011). In the case of a strain-hardening site (e.g. loose to medium-dense sand or normally consolidated clay deposit), the natural vibration frequency of the foundation system is expected to increase, whereas for a strain-softening site (e.g. dense sand or overconsolidated clay deposit), its natural frequency of vibration would decrease (Bhattacharya *et al.*, 2011, 2013).

### 9. Limitations of this study

The present investigation was performed using a model pile, partially embedded in dense sand beds (density index range of 70–74%). Additional testing should be undertaken to evaluate the behaviour of the monopile for other density ranges and different soils types. Further, the field stress conditions can be simulated more adequately within the soil mass (beds) using a centrifuge testing facility, rather than performing the tests at 1g.

It may be a limitation of this study that only 6000 load cycles were applied in some of the tests performed, because the number of load cycles considered for the fatigue limit state of an offshore wind-turbine foundation is significantly greater (Germanischer Lloyd, 2005). It was found that the general trend in the monopile behaviour under cyclic lateral loading had practically stabilised by the 6000th load cycle; that is, although the monopile continues to rotate for greater numbers of load cycles, the experimental data plots presented indicate that this occurs at a decreasing rate. Any quick change in the experimental curve describing the rotation against number of load cycles relationship, as occurred during the first 500 load cycles applied, seems unlikely.

The model pile used in this investigation geometrically represents the field monopile at a scale of approximately 1:100. Among other technical difficulties encountered in performing physical tests with geomaterials, the direct scaling of the particle (grain) dimensions is particularly problematic. Undesirable forces may be introduced unless a certain minimum ratio is maintained between the effective grain size  $d_{50}$  and a characteristic dimension of the model (pile diameter for the present investigation) (Sedran *et al.*, 2001; Verdure *et al.*, 2003). Examples of the derivation of scaling laws for monopile foundation testing at 1g have been reported by Lai (1989), Muir Wood *et al.* (2002), LeBlanc *et al.* (2010), Bhattacharya *et al.* (2011) and Cuéllar *et al.* (2012), although the satisfaction of such scaling conditions for similarity in granular soils, and scaling issues related to the stress field corresponding to homologous points, is not trivial (Bhattacharya *et al.*, 2011; Dong *et al.*, 2001).

### 10. Conclusions

The improvement in performance produced by the piled-cruciform attachment to the monopile head was investigated for many thousands of lateral load cycles. Based on the results of the different series of tests presented, the following conclusions can be drawn.

- (a) The accumulated rotation of the monopile was dependent on the cyclic load characteristics, the embedment depth and inclination of the SDPs and the loading direction orientation (i.e. orientation of the cruciform arms relative to the line of action of the applied loading).
- (b) For four vertical SDPs having  $L_{SDP}/L$  values of 0.33 and 0.5, the greater reduction in monopile rotation at 6000 load cycles was recorded for unbalanced two-way loading (82% and 86%, respectively), followed by partial one-way loading (73% for both), balanced two-way loading (57% and 68%, respectively) and finally one-way loading (24% and 31%, respectively). The performance of the piled-cruciform modification reduced when the cruciform arms were offset by 45° from the line of action of the applied loading.
- (c) The monopile rotation reduced for greater embedment of the SDPs, although for the  $L_{SDP}/L$  values of 0.33 and 0.5 investigated, comparable overall reductions in the monopile rotation were achieved for the experimental conditions investigated. Hence, the shorter SDPs (i.e. one-third of the monopile length) may be adequate for practical purposes.
- (d) Vertical SDPs were more efficient in reducing the accumulated rotation of the monopile compared with SDPs inclined at 15°, 25° and 45° (the last of these was the least efficient among those investigated) to the vertical direction.

For the prototype, the cruciform arms have to be strong and stiff enough to transmit the forces and the monopile will possibly require some strengthening near the head level (possibly achieved through increased wall thickness of the monopile) to avoid buckling.

### Acknowledgement

The first author gratefully acknowledges a postgraduate research award received from Trinity College Dublin.

### REFERENCES

- Achmus M (2010) Design of axially and laterally loaded piles for the support of offshore wind energy converters. *Proceedings of the Indian Geotechnical Conference GEOTrendz, Mumbai, India*, pp. 92–102.
- Achmus M, Kuo YS and Abdel-Rahman K (2009) Behavior of monopile foundations under cyclic lateral load. *Computers and Geotechnics* **36**(5): 725–735.
- Adhikari S and Bhattacharya S (2011) Vibrations of wind-turbines considering soil-structure interaction. *Wind and Structures* **14**(2): 85–112.

- API (American Petroleum Institute) (2010) *API RPA2: Recommended Practice for Planning, Designing and Constructing Fixed Offshore Platforms – Working Stress Design*, 22nd edn. API, Washington, DC, USA.
- Arshad M and O'Kelly BC (2013) Offshore wind-turbine structures: a review. *Proceedings of the Institution of Civil Engineers – Energy* **166(4)**: 139–152.
- Arshad M and O'Kelly BC (2014) Development of a rig to study model pile behaviour under repeating lateral loads. *International Journal of Physical Modelling in Geotechnics* **14(3)**: 54–67.
- Arshad M and O'Kelly BC (2016a) Analysis and design of monopile foundations for offshore wind-turbine structures. *Marine Georesources and Geotechnology*, <http://dx.doi.org/10.1080/1064119X.2015.1033070>.
- Arshad M and O'Kelly BC (2016b) Reducing monopile rotation under lateral loading in sandy soils. *Geomechanics and Geoengineering*, <http://dx.doi.org/10.1080/17486025.2016.1153730>.
- Arshi HS, Stone KJL, Vaziri M *et al.* (2013) Modelling of monopile-footing foundation system for offshore structures in cohesionless soils. *Proceedings of the 18th International Conference on Soil Mechanics and Geotechnical Engineering, Paris, France*, vol. 3, pp. 2307–2310.
- Bhattacharya S and Adhikari S (2011) Experimental validation of soil–structure interaction of offshore wind turbines. *Soil Dynamics and Earthquake Engineering* **31(5–6)**: 805–816.
- Bhattacharya S, Lombardi D and Muir Wood D (2011) Similitude relationships for physical modelling of monopile-supported offshore wind turbines. *International Journal of Physical Modelling in Geotechnics* **11(2)**: 58–68.
- Bhattacharya S, Cox J, Lombardi D and Muir Wood D (2013) Dynamics of offshore wind turbines supported on two foundations. *Proceedings of the Institution of Civil Engineers – Geotechnical Engineering* **166(2)**: 159–169, <http://dx.doi.org/10.1680/geng.11.00015>.
- Bienen B, Dührkop J, Grabe J, Randolph MF and White D (2012) Response of piles with wings to monotonic and cyclic lateral loading in sand. *Geotechnical and Geoenvironmental Engineering* **138(3)**: 364–375.
- Broms BB (1964) Lateral resistance of piles in cohesionless soils. *Journal of the Soil Mechanics and Foundation Engineering Division, ASCE* **90(SM3)**: 123–156.
- Brown DA, Morrison C and Reese LC (1988) Lateral load behavior of pile group in sand. *Journal of Geotechnical Engineering, ASCE* **114(11)**: 1261–1276.
- Carswell W, Arwade SR, DeGroot DJ and Lackner MA (2015) Soil–structure reliability of offshore wind turbine monopile foundations. *Wind Energy* **18(3)**: 483–498.
- Chari TR and Meyerhof GG (1983) Ultimate capacity of rigid single piles under inclined loads in sand. *Canadian Geotechnical Journal* **20(4)**: 849–854.
- Cuéllar P (2011) *Pile Foundations for Offshore Wind Turbines: Numerical and Experimental Investigations on the Behaviour under Short-term and Long-term Cyclic Loading*. PhD thesis, Technical University of Berlin, Berlin, Germany.
- Cuéllar P, Georgi S, Baeßler M and Rucker W (2012) On the quasi-static granular convective flow and sand densification around pile foundations under cyclic lateral loading. *Granular Matter* **14(1)**: 11–25.
- Davie JR and Sutherland HB (1978) Modeling of clay uplift resistance. *Journal of the Geotechnical Engineering Division, ASCE* **104(6)**: 755–760.
- Dickin EA and Laman M (2003) Moment response of short rectangular piers in sand. *Computers and Structures* **81(30–31)**: 2717–2729.
- DNV (Det Norske Veritas) (2011) DNV–OS–J101: Design of Offshore Wind Turbine Structures. DNV, Oslo, Norway.
- Dong P, Newson TA, Davies MCR and Davies PA (2001) Scaling laws for centrifuge modelling of soil transport by turbulent fluid flows. *International Journal of Physical Modelling in Geotechnics* **1(1)**: 41–45.
- Dührkop J and Grabe J (2008) Improving the lateral bearing capacity of monopiles by welded wings. *Proceedings of the 2nd BGA International Conference on Foundations (ICOF 2008)*, Dundee, UK (Brown MJ, Bransby MF, Brennan AJ and Knappett JA (eds)). IHS BRE Press, Garston, UK, vol. 1, pp. 849–860.
- El Sawwaf M (2006) Lateral resistance of single pile located near geosynthetic reinforced slope. *Geotechnical and Geoenvironmental Engineering* **132(10)**: 1336–1345.
- Germanischer Lloyd (2005) *Guideline for the Certification of Offshore Wind Turbines*. Germanischer Lloyd WindEnergie GmbH, Hamburg, Germany.
- Haiderali A, Cilingir U and Madabhushi G (2013) Lateral and axial capacity of monopiles for offshore wind turbines. *Indian Geotechnical Journal* **43(3)**: 181–194.
- Hu Z, McVay M, Bloomquist D, Herrera R and Lai P (2006) Influence of torque on lateral capacity of drilled shafts in sands. *Geotechnical and Geoenvironmental Engineering* **132(4)**: 456–464.
- Irvine JH, Allan PG, Clarke BG and Peng JR (2003) Improving the lateral stability of monopile foundations. *Proceedings of the International Conference on Foundations: Innovations, Observations, Design and Practice, Dundee, UK* (Newson TA (ed.)). Thomas Telford, London, UK, pp. 371–380.
- Karthigeyan S, Ramakrishna VVGST and Rajagopal G (2006) Influence of vertical load on the lateral response of piles in sand. *Computers and Geotechnics* **33(2)**: 121–131.
- Kuo YS, Achmus M and Abdel-Rahman K (2012) Minimum embedded length of cyclic horizontally loaded monopiles. *Geotechnical and Geoenvironmental Engineering* **138(3)**: 357–363.
- Lai S (1989) Similitude for shaking table test on soil–structure–fluid model in 1-g gravitational field. *Soils and Foundations* **29(1)**: 105–118.

Arshad, M., and O'Kelly, B.C. (2016) "Piled-cruciform attachment to monopile head reduces deflection". *Proceedings of the Institution of Civil Engineers – Geotechnical Engineering*, Volume 169, Issue Number 4, pages 321–335.  
<http://dx.doi.org/10.1680/jgeen.15.00001>

- LeBlanc C, Houlsby GT and Byrne BW (2010) Response of stiff piles in sand to long-term cyclic lateral loading. *Géotechnique* **60(2)**: 79–90.
- Lombardi D, Bhattacharya S and Muir Wood D (2013) Dynamic soil–structure interaction of monopile supported wind turbines in cohesive soil. *Soil Dynamics and Earthquake Engineering* **49(2013)**: 165–180.
- Malhotra S (2010) Design and construction considerations for offshore wind turbine foundations in North America. In *Proceedings of GeoFlorida 2010: Advances in Analysis, Modeling and Design, Orlando, FL, USA* (Fratta DO, Puppala AJ and Muhunthan B (eds)). ASCE, Reston, VA, USA, Geotechnical Special Publication no. 199, vol. 2, pp. 1533–1542.
- Moayed RZ, Mehdipour I and Judi A (2012) Undrained lateral behavior of short pile under combination of axial, lateral and moment loading in clayey soils. *Kuwait Journal of Science and Engineering* **39(1B)**: 59–78.
- Muir Wood D, Crewe AJ and Taylor CA (2002) Shaking table testing of geotechnical models. *International Journal of Physical Modelling in Geotechnics* **2(1)**: 1–13.
- Nasr AMA (2014) Experimental and theoretical studies of laterally loaded finned piles in sand. *Canadian Geotechnical Journal* **51(4)**: 381–393.
- Nicolai G and Ibsen LB (2014) Small-scale testing of cyclic laterally loaded monopiles in dense saturated sand. *Journal of Ocean and Wind Energy* **1(4)**: 240–245.
- O'Kelly BC and Arshad M (2016) Offshore wind turbine foundations – analysis and design. In *Offshore Wind Farms: Technologies, Design and Operation* (Ng C and Ran L (eds)). Woodhead Publishing, Cambridge, UK, ch. 20, pp. 589–610.
- Peng J, Clarke B and Rouainia M (2011) Increasing the resistance of piles subject to cyclic lateral loading. *Geotechnical and Geoenvironmental Engineering* **137(10)**: 977–982.
- Prasad YVSN and Chari TR (1999) Lateral capacity of model rigid piles in cohesionless soils. *Soils and Foundations* **39(2)**: 21–29.
- Rao SN, Ramakrishna VGST and Raju GB (1996) Behavior of pile-supported dolphins in marine clay under lateral loading. *Journal of Geotechnical Engineering, ASCE* **122(8)**: 607–612.
- Rosquoët F, Thorel L, Garnier J and Canepa Y (2007) Lateral cyclic loading of sand-installed piles. *Soils and Foundations* **47(5)**: 821–832.
- Sedran G, Stolle DFE and Horvath RG (2001) An investigation of scaling and dimensional analysis of axially loaded piles. *Canadian Geotechnical Journal* **38(3)**: 530–541.
- Stone K, Newson T and Sandon J (2007) An investigation of the performance of a 'hybrid' monopile-footing foundation for offshore structures. In *Proceedings of the 6th International Conference on Offshore Site Investigation and Geotechnics, London, UK*. Society for Underwater Technology, London, UK, pp. 391–396.
- Terzaghi K (1955) Evaluation of coefficients of subgrade reaction. *Géotechnique* **5(4)**: 297–326.
- Tomlinson MJ (2001) *Foundation Design and Construction*, 7th edn. Pearson, Harlow, UK.
- Uncuoğlu E and Laman M (2011) Lateral resistance of a short rigid pile in a two-layer cohesionless soil. *Acta Geotechnica Slovenica* **8(2)**: 19–43.
- Verdure L, Garnier J and Levacher D (2003) Lateral cyclic loading of single piles in sand. *International Journal of Physical Modelling in Geotechnics* **3(3)**: 17–28.
- Zhang L, Silva F and Grismala R (2005) Ultimate lateral resistance to piles in cohesionless soils. *Geotechnical and Geoenvironmental Engineering* **131(1)**: 78–83.
- Zhu B, Byrne BW and Houlsby GT (2013) Long-term lateral cyclic response of suction caisson foundations in sand. *Geotechnical and Geoenvironmental Engineering* **139(1)**: 73–83.

#### WHAT DO YOU THINK?

To discuss this paper, please email up to 500 words to the editor at [journals@ice.org.uk](mailto:journals@ice.org.uk). Your contribution will be forwarded to the author(s) for a reply and, if considered appropriate by the editorial panel, will be published as discussion in a future issue of the journal.

*Proceedings* journals rely entirely on contributions sent in by civil engineering professionals, academics and students. Papers should be 2000–5000 words long (briefing papers should be 1000–2000 words long), with adequate illustrations and references. You can submit your paper online via [www.icevirtuallibrary.com/content/journals](http://www.icevirtuallibrary.com/content/journals), where you will also find detailed author guidelines.